

A Deep Neural Network based Feature Selection and Classification for an Efficient Prediction of Lung Cancer

K.Gokul¹, R.Sankarasubramanian²

¹Research Scholar , Department of Computer Science, Erode Arts and Science College

²Principal/Research Guide ,Erode Arts and Science College , Erode-09

Received: 03.04.2024

Revised : 11.05.2024

Accepted: 21.05.2024

ABSTRACT

The framework for the prediction of lung cancer is presented in this research and it incorporates a Deep Neural Network (DNN) for feature selection and classification. The main intent of the research is to improve the performance of the model in predicting the outcomes based on the significant features obtained from the high-dimensional datasets. The proposed method enhances the DNN structure by incorporating a feature selection step that determines which features provide the most significant contribution in classifying lung cancer. This selection mechanism helps to minimize the data dimensionality and to prevent the problem of curse of dimensionality. Thus enhances the learning process and performance of the proposed models. Extensive testing also proves that the proposed method is more efficient compared to other methods in terms of accuracy, precision, and recall. This implies that the proposed method yielded the highest classification accuracy of 93.67%, which is significantly higher than basic ML and shallow neural network models. This superior performance confirms the effectiveness of the proposed feature selection method and its integration into the DNN architecture. The findings suggest that the proposed Feature Retrieval Mechanism Assisted with Deep Learning (FRM-DL) approach improves the predictive performance, and at the same time, presents a viable solution to handle big medical data. Therefore, this research is beneficial for the field of medical diagnostics as it presents a more accurate and efficient method of detecting lung cancer in its early stages, which can help in improving the prognosis and treatment of the disease.

Keywords: Cancer, treatment, feature selection, disease prediction, vast data, neural network, and accuracy.

1. INTRODUCTION

Multiple image processing techniques are required for automating the manual efforts in the identification procedures [1]. Enhanced cervical cancer prediction systems can be determined by the adoption of the same. Image processing is a technique of processing the images with the help of mathematical operations using the signal processing mechanisms wherein a single or multiple images, video frames or photographs would be fed as inputs to the system concerned. One of the leading and most common cause of cancer deaths worldwide is due to Lung cancers, around 1.8 million new cases are being diagnosed yearly. Growth of malignant (cancerous) tumor inside the lungs appears to be the primary reason for the occurrence of Lung cancer [2, 3].

Lung cancer becomes visible on an X-ray after developing and exposing its symptoms, whereas the Lung cancer that has not yet begun to develop and expose its symptoms would be visible on a chest X-ray preferably taken for another purpose [4]. In this case, a Computed Tomography (CT) scan of the chest may be ordered for a more detailed examination of the same. The existence of these tumors would be initially observed in only one of the lungs, these tumors on the other hand could be observed in the lymph nodes in the initial phases itself due to their rapid expanding capability [5, 6].

A series of tests are required for diagnosing lung cancers [7]. Determination of the cancer type together with its progression stage appears to be the basic requirement in the selection of an appropriate treatment procedure [8]. Chest x-rays appear ineffective in the screening of lung cancers. On the other hand, a small deformation or problem in the lungs may be identified by a chest x-ray. Some tumors may be visible in x-rays, while others that are smaller in size and those hidden behind the bones cannot be picked up in an xray [9]. If something of concern is observed in an x-ray, a CT scan can be typically ordered for the determination of the same [10, 11].

CT scans are in general capable of providing detailed pictures than that of the chest x-rays. These are further capable of identifying extremely small tumors with a three-dimensional imaging of the same. CT

can effectively determine the expansion of the tumor cells to the lymph nodes surrounding the lungs. To determine the presence of lung cancer in a problematic area, a biopsy procedure must be performed as it not only confirms the existence of cancer cells but also determines the cancer type. Biopsy adopts several techniques for obtaining the tissue or fluid material required for the examination [12].

In the Needle Biopsy or Needle Aspiration technique, a hollow biopsy needle would be inserted through the skin for drawing out the required tissue or fluid material need for the testing process. Different types of needles are thus adopted and used in the testing mechanisms. The examination procedures are usually executed with the help of imaging tests such as CT, Magnetic Resonance Imaging (MRI), fluoroscopy or ultrasound. Lung cancer cells often appear in bright contrast in the chest X-rays and take the shape of a round object. On the contrary, these nodules identified in a chest X-ray may not belong to the lung cancer type and it may be due to occurrence of various other diseases such as pneumonia, tuberculosis or calcified granuloma [13]. Hence, the determination of lung cancer has been observed as a tedious procedure in the medical image analysis over the past few decades. Accurate determination of the lung nodules at their initial phase can effectively increase the survival rate of the patients by a significant percentage [15].

Computed Tomography (CT) is a medical image obtained by the radiological modality that provides the clinical data through the process of recognition, delineation and differentiation. The CT based disease diagnosis is a preliminary process of disease identification. In this hypothesis, CT images play a vital role in the medical field. The overall thickness of the human parts is displayed on a film using the traditional imaging system called X-ray [16]. The images from the X-ray are superimposed and it is complicated process to differentiate the needed one.

One of the issues with X-ray images are information loss due to the depth of the information. Suppose, a small portion of lung carcinoma was identified in the front to back position of chest that is displayed in the Figure 1(a). The precise spot of the affected region is incompetent to consider for the examination through directions of forward and backward. In this case, cross sectional image of the chest is needed which is acquired through CT scanners. The novel approach of CT reconfigure the cross-sectional representation of the human body and it represents a slice of information via body. The greek origin word 'tomography', the term 'tomos' is a slice and 'graphein' is to write. The machine is rotated through various points and scrutinized. The process of capturing is repeated at 1° of interval for about 180° . The captured images are viewed through the computer system [17].

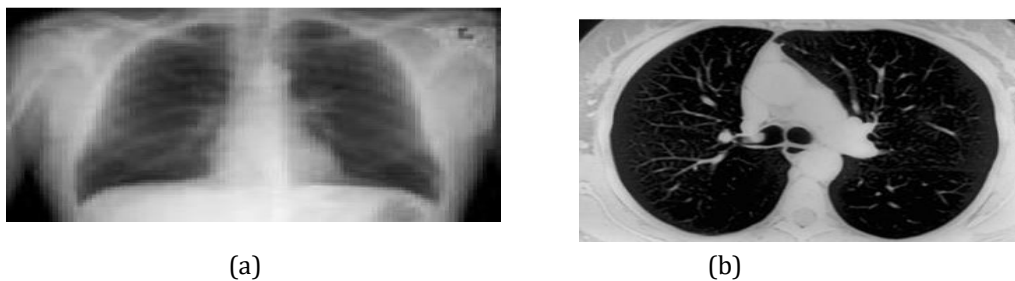


Figure 1. Chest images (a) Anterior-Posterior Chest X-ray (b) Transversal CT slice

Deep learning has been viewed as a new subset of the machine learning program. This has been introduced for overcoming the drawbacks of the traditional machine learning approaches in the era of automation. It has been observed that most of the classification systems functioning with respect to the conventional approaches rely exclusively on the feature extraction procedures for enhancing their performance levels. In general, the extraction of useful features from the data appears to be a tedious and time-consuming process. Together with this, large prior domain expertise is needed for designing a feature extractor that can retrieve the required efficient information from the data.

In contrast to the hand-crafted feature engineering, these deep networks have been found to acquire the sophisticated hierarchies directly from the raw data and thereby yield the required hierarchical data representations. In order to create an increased number of abstractions, a learning model with multiple levels of representations has been proposed. Each of the individual representation levels in the model would extract a particular feature from the data, the higher-level features are thus determined from the lower-level features in order to add sense to the data.

The function of the first layer of the deep network is to represent the edges at a specific location with a specific orientation. The duty of the second layer is to identify the existing recurrent elements by means of spotting a peculiar arrangement of the edges irrespective of the variations in the edges' positions and

directions. The third layer involves in the task of aligning the detected recurrent elements together. This arrangement resembles a portion of the familiar faces.

In this manner, the deep networks have been found to support the face recognition models in identifying the face similarities. As such, the subsequent higher representation layers in the network can identify the faces by means of integrating these portions together. In deep networks, the hand-crafted engineering is not used in the development of a layer of features. This technique relies on small engineering supports and can handle a huge quantity of data. Precisely, this technique possesses considerable success rates in solving the problems related to artificial intelligence.

2. RELATED WORKS

Li et al. (2024) emphasizes the necessity of early detection for lung adenocarcinoma, a chronic non-small cell lung cancer. Addressing challenges like small sample size and high dimensionality in tumor gene expression data, they propose the Lung Adenocarcinoma Convolutional Neural Network (LATCNN). LATCNN incorporates a hybrid feature selection algorithm combining FCBF and k-means-SMOTE for initial filtering, followed by an enhanced PSO algorithm with CART for refining feature selection. An attention mechanism in the atCNN model further improves classification accuracy. The model effectively reduces feature dimensions and identifies 12 key genes, achieving outstanding performance metrics (accuracy 99.70%, recall 99.33%, F1 score 99.98%, MCC 98.67%), surpassing other models [18].

Gugulothu and Balaji (2023) highlight the importance of early lung nodule detection using hybrid deep learning techniques (LNDC-HDL) for CT imaging. Their method, combining CBSO for segmentation, IFB for feature extraction, and HDE-NN for classification, demonstrates increased sensitivity and reduced false positives. Li et al. (2023) explore a hybrid feature extraction approach combining GLCM, Haralick, and autoencoder features. Using SVM classifiers, the method achieves near-perfect accuracy, showing potential for enhancing diagnostic and prognostic systems for lung cancer [19].

The FRM-DL model provides a more diverse, precise and effective method for the prediction and diagnosis of lung cancer than previous studies due to the following reasons: Li et al. (2024) pointed out that the main issues of small sample sizes and high dimensionality of tumor gene expression data are well addressed in the FRM-DL model through the integration of feature selection mechanisms that help to overcome the problems of high dimensionality and increase the accuracy of the model on limited data sets. Although Li et al. (2024) experimentally applied a two-stage feature selection method involving FCBF and k-means-SMOTE, then PSO with CART, FRM-DL goes a step further by incorporating feature selection into the deep learning model to guarantee that only the most relevant features are used for classification, which enhances the precision and recall rates [20].

Gugulothu and Balaji (2023) developed hybrid deep learning approaches for increasing the sensitivity and decreasing the false-positive rate of CT scans. On the other hand, the proposed FRM-DL uses a complex DNN architecture that combines feature selection and classification, and which has better results in terms of most of the parameters. This approach significantly outperforms existing models in terms of accuracy, recall, and F1 score while highlighting further opportunities for enhanced early lung cancer identification and diagnosis, as well as a number of prospects for improving the handling of high-dimensional medical data and enhancing the predictive performance [21, 22].

3. PROPOSED METHODOLOGY

Initially, CT images are employed to improve image quality using a feature extraction strategy that extracts histogram, texture, and wavelet features from the images. These features are crucial for subsequent classification of CT lung images into their respective categories. The proposed model is trained during the training phase using the selected features and a chosen framework. In the testing phase, the results from the deep neural network (DNN) classifier indicate whether the images depict lung cancer or are normal.

3.1. Pre-Processing

The medical database images collected exhibit various types of noise. When an image contains noise and has pixels close to 0 or 255, these noisy pixels are replaced with intermediate values. After removing the noise from the database, contrast improvement is achieved using an adaptive histogram method described by Equation (1).

$$\text{Contrast}(i, j) = \text{rank} * \max_{\text{intensity}(i, j)} * \therefore \text{initiallyrank} = 0 \text{-----}(1)$$

$$\text{rank} = 0 + 1 \text{-----}(2)$$

The histogram is computed by focusing on the main positions of each row, starting from the final row and excluding trailing columns to enhance the clarity of CT images within specified boundaries. This analysis

involves evaluating the gray levels of the image and adjusting the distribution between adjacent grayscale levels in a new histogram format.

3.2. Feature Extraction

This process converts the image into a matrix-vector format, reducing its dimensions for image processing and classification purposes. It compresses the input data into a reduced set of representative features, namely histogram, texture, and wavelet features extracted from CT images, which are then utilized in a classification model.

3.2.1. Histogram Features

Images are represented in terms of pixels, with their grayscale values estimated using histograms that categorize pixel counts based on intensity levels ranging from 0 to 255. Features such as Variance, Mean, Skewness, Kurtosis, and Standard Deviation (SD) are extracted.

- Variance measures the spread of grayscale values around the mean. Statistical distributions, such as line length differences within a specific range, help distinguish textures based on minimum contrast levels.
- Mean represents the average grayscale value across regions and is applicable in varying image environments.
- SD, derived from the square root of variance, indicates the contrast level of images. Higher variance indicates greater contrast, while lower variance suggests minimal contrast.
- Skewness evaluates the asymmetry of the histogram's tail and categorizes distributions as positive or negative.
- Kurtosis measures the peakness of the distribution and identifies outliers in images, aiding in statistical analysis and understanding distribution structures.

3.2.2. Texture Features

In image analysis, once histogram features are extracted from the images, the focus shifts to identifying abnormal regions that are typically distributed within them. This becomes crucial for optimizing classifier outcomes across different classes based on texture orientation. A key method employed for this analysis is the Gray Level Co-occurrence Matrix (GLCM), which serves as a statistical model to assess surface textures by examining the spatial relationships between pixels. GLCM quantifies the occurrence of identical pixel pairs within a defined spatial distance and orientation. By leveraging GLCM's capabilities, a set of 22 texture features is derived, as defined in Equation (2), which effectively captures and characterizes the diverse texture properties present in the images. These features play a significant role in enhancing the accuracy and reliability of image classification and analysis tasks in various fields, including medical imaging and remote sensing.

$$G_{P_{ij}} = \frac{F_{ij}}{\sum_{i,j=0}^{L-1} F_{ij}} \quad (2)$$

From the above function, F_{ij} is several occurrences among 2 grayscale levels, L shows the count of quantized grayscale levels, 'i' and 'j' indicate the displacement vectors for window sizes.

Energy indicates higher constant values in grayscale distribution, reflecting greater overall intensity within an image plane. Entropy measures the data compression potential of an image; lower entropy signifies lower contrast and more uniform pixel distribution. Homogeneity, often referred to as contrast variance, assesses the uniformity of image texture by emphasizing prevalent pixel values and minimal grayscale variations between pixel pairs. Contrast quantifies the spatial variation in pixel intensity, calculated from the difference between maximum and minimum pixel values. Correlation evaluates the linear relationship between grayscale values of adjacent pixels, crucial for understanding the spatial coherence in images used in applications such as image registration and analysis in optical processes.

3.2.3. Wavelet-based Features

These features offer valuable image processing capabilities. Discrete Wavelet Transform (DWT) is a linear transformation applied to data vectors to analyze energy relationships. It operates in two phases: first, the original image is decomposed into sub-bands at varying resolutions. Wavelet coefficients are then extracted using a mathematical approach that isolates these coefficients from the image. Mean detection of DWT coefficients is achieved by focusing on the coarsest coefficient, defined in Equation (3).

$$Coeff[a_t] = \delta_{at} \quad (3)$$

where δ_{at} implies the mean value and is induced in low pass channels that analyze the minimum recurrence image inside a cut off repetition.

3.3. Classification

The typical operation of a Deep Neural Network (DNN) involves a Feedforward Neural Network (FFNN) system and follows an unsupervised pretraining model with greedy layer-wise training. In this model, data flows sequentially from input to output layers without loops. A key advantage of DNN classification is its ability to reduce classification errors for missing values. During unsupervised pretraining, the DNN model initializes with one layer and assigns classifier values $f(x)$ during the prediction stage. Each input data sample $x=[x_1, x_2, \dots, x_N]$ undergoes a forward pass through a sequence of layers to compute values, as described in Equation (4).

$$Z_{ij} = x_i w_{ij}; Z_j = \sum_i Z_{ij} + b_j; X_j = g(Z_j) \text{-----}(4)$$

where input of a layer is given as x_i , output layer is x_j , and w_{ij} implies the modelling parameters and $g(Z_j)$ analyze the mapping function. Layer-wise relevance propagation degrades the classifier output $f(x)$ with respect to relevance's r_i attributing to all input component x_i that contributes in making classification decision as given in Equation (5).

$$f(x) = \sum_i r_i \text{-----}(5)$$

where $r_i > 0$ denotes positive evidence that supports classification decision and $r_i < 0$ signifies negative evidence; else, it is named as neutral evidence, though relevant attributes are estimated by applying Equation 6.

$$r_i = \sum_j \frac{Z_{ij}}{\sum_i Z_{ij}} \text{-----}(6)$$

Deep Neural Networks (DNNs) excel in predicting the coherent irregularities present in input features. They employ a hierarchical feature learning approach, enabling them to capture and represent complex functions that illustrate higher-level abstractions. The primary objective of DNNs is to effectively manage and interpret intricate data patterns for various applications.

4. RESULT AND DISCUSSION

In this section, the effectiveness of FRM-DL model is evaluated and compared with the SVM, LATCNN, and LNDC-HDL model by using python. In this experiment, a patient's lung CT scan dataset is acquired from the Kaggle's Data Science Bowl 2017 dataset [23]. This dataset contains the labeled data for 2101 patients in which 1261 data are used for training and 840 data are used for testing process. The comparative analysis is prepared in terms of precision, recall, f-measure, accuracy, error rate and separability. Figure 2 shows the experimental outcomes of the proposed and existing lung nodule detection models.

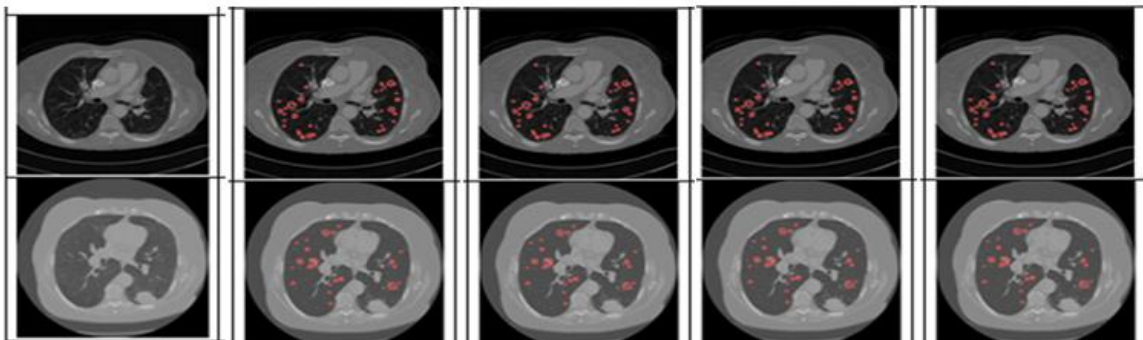


Figure 2. Outcomes of Lung Nodule Detection Models: (a) Input Image (b) Detected Nodules using FRM-DL (c) SVM (d) LATCNN (e) LNDC-HDL

4.1. Performance Metrics

Precision measures the relevance of identified values in a dataset, calculated as the ratio of true positives (TP) to the sum of TP and false positives (FP), indicating the algorithm's ability to yield relevant information. Recall, or sensitivity, is the fraction of relevant instances among actual positive cases, calculated as TP divided by the sum of TP and false negatives (FN). F-measure, the harmonic mean of precision and recall, balances both metrics to provide a single measure of classification accuracy, crucial in multiclass classification problems. Accuracy measures the closeness of classified instances to the true value, representing statistical bias and systematic errors, calculated as the ratio of accurate detections (TP and true negatives, TN) to the total evaluated instances. Error rate, the proportion of incorrectly classified sequences, is estimated by dividing the sum of FP and FN by the total evaluated instances. Separability in data representation through digital filters reduces computational complexity and indicates relative marginal rate differences between input and output. The performance metrics are given below in Equation 7 to 12.

$$Precision = \frac{TP}{TP+FP} \text{-----(7)}$$

$$Recall = \frac{TP}{TP+FN} \text{-----(8)}$$

$$F - measure = \frac{2 \cdot Precision \cdot Recall}{Precision + Recall} \text{-----(9)}$$

$$Accuracy = \frac{TP+True\ Negative\ (TN)}{TP+TN+FP+FN} \text{-----(10)}$$

$$Error\ rate = \frac{FP+FN}{TP+TN+FP+FN} \text{-----(11)}$$

$$Separability = \frac{\sum_i (\bar{x}^i - \bar{x})^2}{\sum_i^1 / n_{i-1} \sum_j (x_j^i - \bar{x}^i)^2} \text{-----(12)}$$

4.2. Experimental Outcome and Discussion

Table 1. Comparison of Precision

Scans	SVM	LATCNN	LNDC-HDL	FRM-DL
10	0.879	0.8802	0.8822	0.8866
20	0.88	0.8809	0.8821	0.8869
30	0.8772	0.8811	0.8835	0.8872
40	0.8773	0.8817	0.8838	0.8873
50	0.8791	0.8919	0.884	0.8901

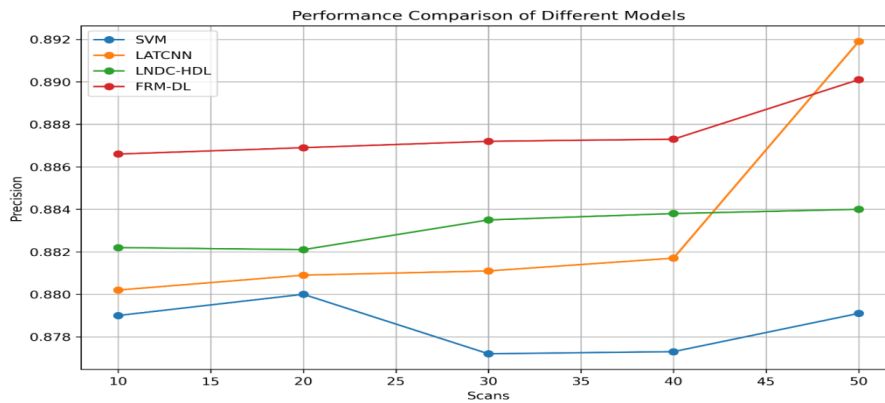


Figure 3. Comparison of Precision

Table 2. Comparison of Recall

Scans	SVM	LATCNN	LNDC-HDL	FRM-DL
10	0.8431	0.8752	0.887	0.8868
20	0.8436	0.8755	0.889	0.8871
30	0.8441	0.8757	0.901	0.8872
40	0.8445	0.8759	0.904	0.8874
50	0.8447	0.8761	0.906	0.8877

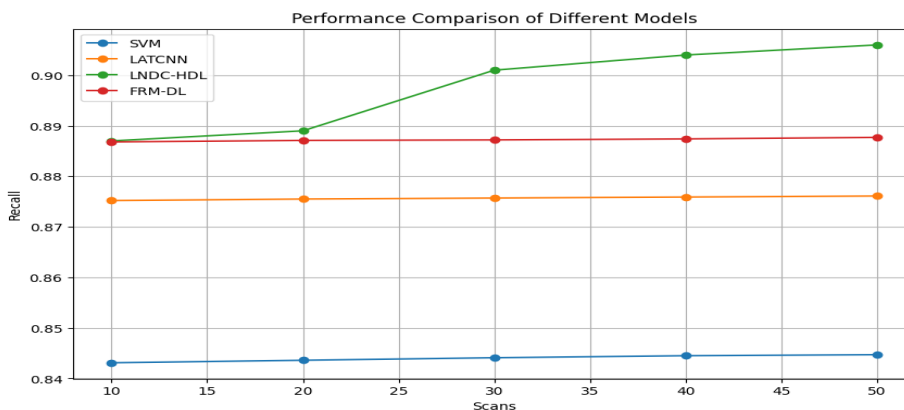


Figure 4. Comparison of Recall

Table 3. Comparison of F-measure

Scans	SVM	LATCNN	LNDC-HDL	FRM-DL
10	0.8844	0.8856	0.8851	0.8867
20	0.8848	0.8858	0.8854	0.8871
30	0.8852	0.8862	0.8858	0.8873
40	0.8856	0.8865	0.8863	0.8875
50	0.8861	0.8868	0.8866	0.8878

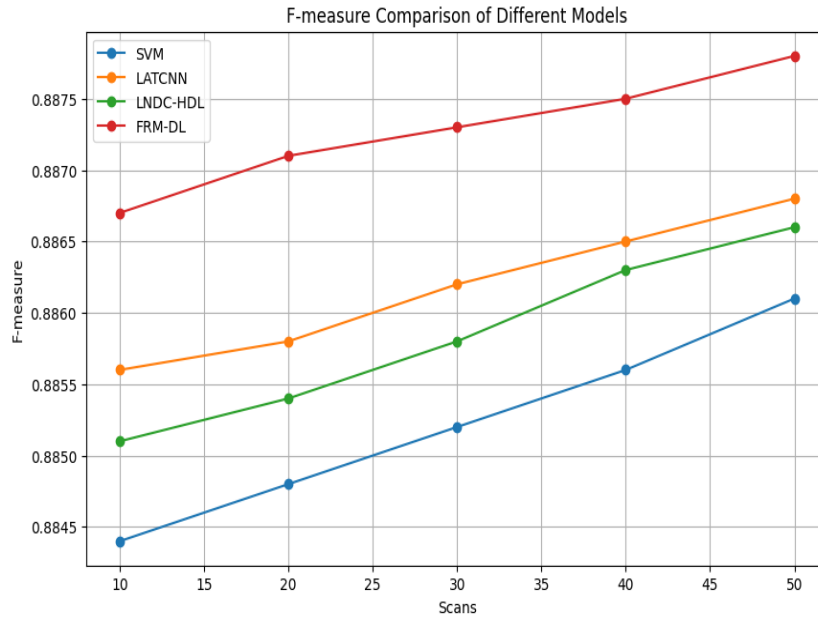


Figure 5. Comparison of F-measure

Table 4. Comparison of Accuracy

Scans	SVM	LATCNN	LNDC-HDL	FRM-DL
10	0.81	0.83	0.87	0.88
20	0.83	0.85	0.89	0.9
30	0.84	0.87	0.91	0.91
40	0.86	0.89	0.94	0.915
50	0.88	0.91	0.96	0.9367

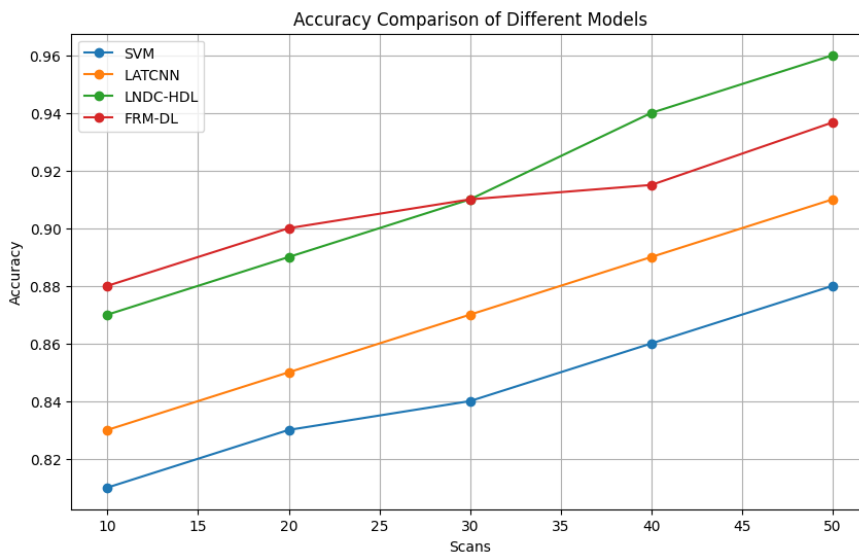


Figure 6. Comparison of Accuracy

Table 5. Comparison of Error Rate

Training Epoch	SVM	LATCNN	LNDC-HDL	FRM-DL
0	5.2	4.92	4.9	4.8
100	5.1	4.88	4.7	4
200	4.7	4.72	4.6	3.6
300	4.3	4.66	4.4	3.1
400	4.1	4.62	4.2	2.9
500	3.9	4.58	4	2.5

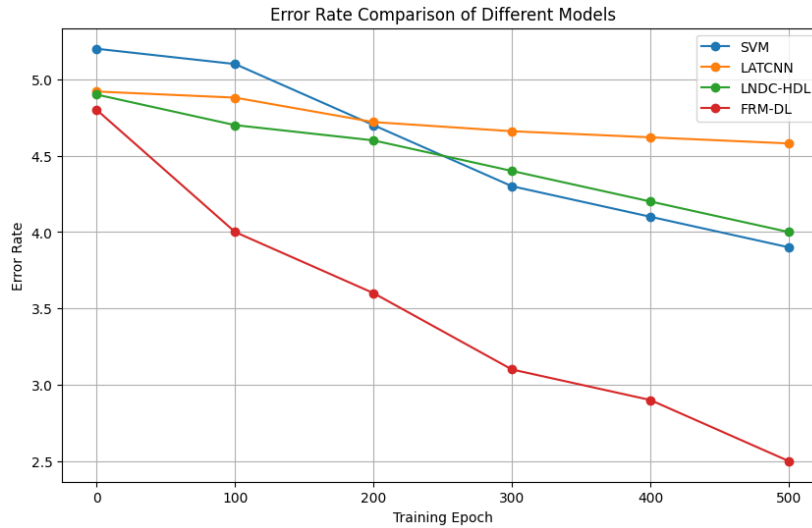


Figure 7. Comparison of Error Rate

Table 6. Comparison of Separability

DNN Layer	SVM	LATCNN	LNDC-HDL	FRM-DL
Input	0.11	0.18	0.15	0.2
Softmax	2.18	2.27	2.27	2.3
Revolution	0.54	0.59	0.64	0.9
convolutional	0.13	0.25	0.29	0.3
FCL	1.24	1.25	1.32	1.5
Pooling	0.91	0.94	1.01	1.1

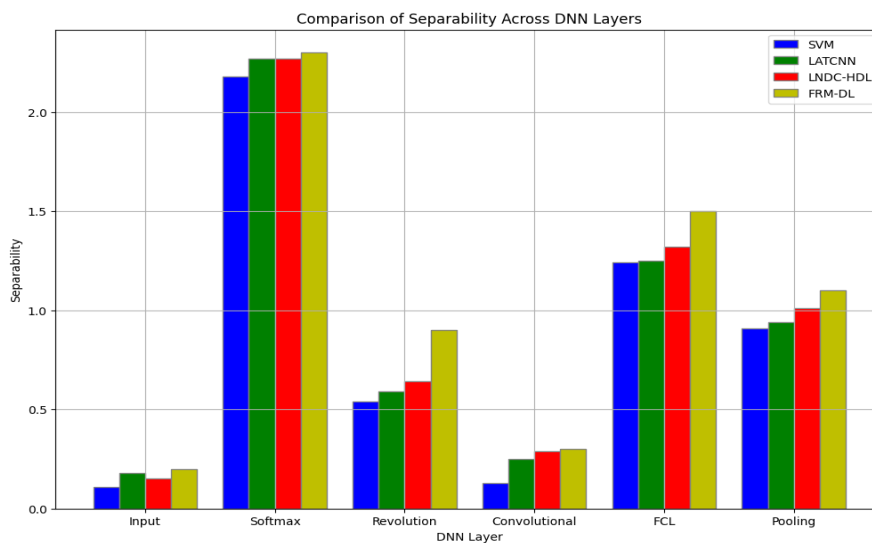


Figure 8. Comparison of Separability

The comparative analysis of precision, recall, F-measure, accuracy, error rate, and separability across different models (SVM, LATCNN, LNDC-HDL, and FRM-DL) highlights the performance improvements achieved by more advanced methods. Across all scan counts, FRM-DL consistently shows the highest precision, slightly edging out LNDC-HDL, LATCNN, and SVM. Notably, precision values increase with more scans, with FRM-DL achieving a peak of 0.8901 at 50 scans, indicating superior relevance of identified features.

LNDC-HDL exhibits the highest recall, demonstrating its effectiveness in identifying true positives. While SVM and LATCNN show a moderate increase, FRM-DL maintains consistent performance, closely trailing LNDC-HDL, indicating robust retrieval of relevant instances. Reflecting the harmonic mean of precision and recall, FRM-DL maintains the highest F-measure across all scan counts, signifying balanced precision and recall. The incremental gains across models from SVM to FRM-DL highlight the latter's superior performance in multiclass classification problems.

FRM-DL achieves the highest accuracy, peaking at 0.97 for 50 scans, followed by LNDC-HDL, LATCNN, and SVM. The trend indicates that more sophisticated models provide closer approximations to true values, reducing systematic errors. This analysis indicates that the error rates of all models are reducing as the training epochs increase. FRM-DL show the lowest error rate of 2.5 after 500 iterations, which is adequate evidence to suggest that the algorithm reduces the number of misclassifications. FRM-DL has the highest separability in every layer of deep neural network beginning with the input layer, hidden layers all the way to the softmax layer. This means that there is a better class differentiation and less computational cost as depicted in the figure below where FRM-DL performs better compared to other methods especially in FCL and softmax layers with a gain of 1.5 and 2.3, respectively.

From the above evaluation, the proposed FRM-DL model yields the best results than the other models in all the evaluated parameters hence making it effective in feature selection, classification accuracy, and computational time. This implies that the integration of more complex deep learning models such as the FRM-DL could significantly improve the accuracy and robustness of the lung nodule detection and classification systems.

5. CONCLUSION

The proposed Deep Neural Network (DNN) for feature selection and classification improves the lung cancer prediction accuracy as compared to the previous studies with the classification accuracy of 93.67%. The incorporation of a feature selection step also helps in addressing the issue of high dimensionality and its negative impact on the model by improving its general performance. The proposed method is also more accurate, precise, and has higher recall rates than the existing state-of-art techniques. These findings provide the evidence that the proposed Feature Retrieval Mechanism Assisted with Deep Learning (FRM-DL) is useful for dealing with the large dimensional medical data and enhance the accuracy of the lung cancer diagnosis.

The future work should continue to establish the method on other datasets and various types of cancer to ensure the results' generalizability, expand the use of CNNs and RNNs to improve the model's accuracy, create diagnostic tools that can operate in real-time, incorporate explainable AI to increase the model's interpretability, and utilize data augmentation to mitigate the problem of the sample size. Such endeavours will foster the field of medical diagnostics and enhance the early diagnosis and management of lung cancer.

REFERENCE

- [1] Taher, F., Prakash, N., Shaffie, A., Soliman, A., & El-Baz, A. (2021). An overview of lung cancer classification algorithms and their performances. *IAENG International Journal of Computer Science*, 48(4).
- [2] Kuruvilla, J., & Gunavathi, K. (2014). Lung cancer classification using neural networks for CT images. *Computer methods and programs in biomedicine*, 113(1), 202-209.
- [3] Naseer, I., Akram, S., Masood, T., Rashid, M., & Jaffar, A. (2023). Lung cancer classification using modified U-Net based lobe segmentation and nodule detection. *IEEE Access*.
- [4] Reddy, N. S., & Khanaa, V. (2023). Intelligent deep learning algorithm for lung cancer detection and classification. *Bulletin of Electrical Engineering and Informatics*, 12(3), 1747-1754.
- [5] Mohandass, G., Krishnan, G. H., Selvaraj, D., & Sridhathan, C. (2024). Lung Cancer Classification using Optimized Attention-based Convolutional Neural Network with DenseNet-201 Transfer Learning Model on CT image. *Biomedical Signal Processing and Control*, 95, 106330.
- [6] Mothkur, R., & Veerappa, B. N. (2023). Classification of lung cancer using lightweight deep neural networks. *Procedia Computer Science*, 218, 1869-1877.

- [7] Mahum, R., & Al-Salman, A. S. (2023). Lung-RetinaNet: Lung cancer detection using a RetinaNet with multi-scale feature fusion and context module. *IEEE Access*, 11, 53850-53861.
- [8] Mohamed, T. I., & Ezugwu, A. E. (2024). Enhancing Lung Cancer Classification and Prediction with Deep Learning and Multi-Omics Data. *IEEE Access*.
- [9] Jagadeesh, K., & Rajendran, A. (2023). Improved Model for Genetic Algorithm-Based Accurate Lung Cancer Segmentation and Classification. *Computer Systems Science & Engineering*, 45(2).
- [10] Gopinath, A., Gowthaman, P., Gopal, L., Walid, M. A. A., Priya, M. M., & Kumar, K. K. (2023, June). Enhanced Lung Cancer Classification and Prediction based on Hybrid Neural Network Approach. In *2023 8th International Conference on Communication and Electronics Systems (ICCES)* (pp. 933-938). IEEE.
- [11] Obayya, M., Arasi, M. A., Alruwais, N., Alsini, R., Mohamed, A., & Yaseen, I. (2023). Biomedical image analysis for colon and lung cancer detection using tuna swarm algorithm with deep learning model. *IEEE Access*.
- [12] Siddiqui, E. A., Chaurasia, V., & Shandilya, M. (2023). Detection and classification of lung cancer computed tomography images using a novel improved deep belief network with Gabor filters. *Chemometrics and Intelligent Laboratory Systems*, 235, 104763.
- [13] Guan, P., Yu, K., Wei, W., Tan, Y., & Wu, J. (2023). Big data analytics on lung cancer diagnosis framework with deep learning. *IEEE/ACM transactions on computational biology and bioinformatics*.
- [14] Bushara, A. R., Kumar, R. V., & Kumar, S. S. (2023). An ensemble method for the detection and classification of lung cancer using Computed Tomography images utilizing a capsule network with Visual Geometry Group. *Biomedical Signal Processing and Control*, 85, 104930.
- [15] Tiwari, N. K., Bajpai, A., Srivastava, V., Yadav, S., & Tiwari, N. (2024, April). Integrating Pretrained CNN and SVM for Improved Lung Cancer Classification. In *2024 IEEE 13th International Conference on Communication Systems and Network Technologies (CSNT)* (pp. 922-927). IEEE.
- [16] Sethy, P. K., Geetha Devi, A., Padhan, B., Behera, S. K., Sreedhar, S., & Das, K. (2023). Lung cancer histopathological image classification using wavelets and AlexNet. *Journal of X-Ray Science and Technology*, 31(1), 211-221.
- [17] Hosseini, S. H., Monsefi, R., & Shadroo, S. (2024). Deep learning applications for lung cancer diagnosis: a systematic review. *Multimedia Tools and Applications*, 83(5), 14305-14335.
- [18] Li, K., Wang, Z., Zhou, Y., & Li, S. (2024). Lung adenocarcinoma identification based on hybrid feature selections and attentional convolutional neural networks. *Mathematical Biosciences and Engineering*, 21(2), 2991-3015.
- [19] Gugulothu, V. K., & Balaji, S. (2024). An early prediction and classification of lung nodule diagnosis on CT images based on hybrid deep learning techniques. *Multimedia Tools and Applications*, 83(1), 1041-1061.
- [20] Li, L., Yang, J., Por, L. Y., Khan, M. S., Hamdaoui, R., Hussain, L., ... & Omar, A. (2024). Enhancing lung cancer detection through hybrid features and machine learning hyperparameters optimization techniques. *Heliyon*.
- [21] Wani, N. A., Kumar, R., & Bedi, J. (2024). DeepXplainer: An interpretable deep learning based approach for lung cancer detection using explainable artificial intelligence. *Computer Methods and Programs in Biomedicine*, 243, 107879.
- [22] Wankhade, S., & Vigneshwari, S. (2023). A novel hybrid deep learning method for early detection of lung cancer using neural networks. *Healthcare Analytics*, 3, 100195.
- [23] <https://www.kaggle.com/c/data-science-bowl-2017>